REPORT DOCUMENTATION PAGE

1a	AD-A231 675	1b. RESTRICTIVE MARKINGS
2a		3. DISTRIBUTION / AVAILABILITY OF REPORT
2b. DECLASSIFICATION / DOWNGRADING SCHEDULE		Approved for public release; distribution unlimited

4. PERFORMING ORGANIZATION REPORT NUMBER(S)	5. MONITORING ORGANIZATION REPORT NUMBER(S)
Technical Report # 58	

6a. NAME OF PERFORMING ORGANIZATION	6b. OFFICE SYMBOL (If applicable)	7a. NAME OF MONITORING ORGANIZATION
Dept. of Chemistry George Washington Univ.		Office of Naval Research (Code 418)

6c. ADDRESS (City, State, and ZIP Code)	7b. ADDRESS (City, State, and ZIP Code)
Washington, DC 20052	Chemistry Program 800 N. Quincy Street Arlington, VA 22217

8a. NAME OF FUNDING / SPONSORING ORGANIZATION	8b. OFFICE SYMBOL (If applicable)	9. PROCUREMENT INSTRUMENT IDENTIFICATION NUMBER
Office of Naval Research		Contract N00014-89-J-1103

8c. ADDRESS (City, State, and ZIP Code)	10. SOURCE OF FUNDING NUMBERS			
	PROGRAM ELEMENT NO.	PROJECT NO.	TASK NO. R & T 4134043-01	WORK UNIT ACCESSION NO.
Chemistry Program 800 Nth, Quincy, Arlington, VA 22217				

11. TITLE (Include Security Classification)

CEELS as a Probe of the Carbide to Graphite Transformation on Ni (Unclassified)

12. PERSONAL AUTHOR(S) David E. Ramaker

13a. TYPE OF REPORT	13b. TIME COVERED		14. DATE OF REPORT (Year, Month, Day)	15. PAGE COUNT
Interim Technical	FROM _____	TO _____	January 1991	10

16. SUPPLEMENTARY NOTATION
Prepared for publication in Proc. 2nd Intn. Conf. New Diamond Sci. & Tech. (Materials Res. Soc.)

17.	COSATI CODES		18. SUBJECT TERMS (Continue on reverse if necessary and identify by block number)
FIELD	GROUP	SUB-GROUP	Carbide Nucleation Electron Energy Loss
			Graphite X-ray Absorption

19. ABSTRACT (Continue on reverse if necessary and identify by block number)

Recent effective medium theory calculations indicate that a nucleation step must be involved in the carbide to graphite transformation on Ni, and that vertical C_2 may be a precursor to this nucleation step. A similar nucleation site could also be involved in diamond formation on metals. We interpret previously published C K edge CEELS and NEXAFS data for carbon/Ni between 500-700K. We make comparison with theoretical DOS calculations, and utilize CEELS angle dependencies to assign features and determine bond orientations on the surface. The results confirm that horizontal C_n, most likely C_2, exists on the surface up 600K, but that at 620K, some of the C_2 species flip up. Evidence for vertical C_2 is seen only at higher C coverages suggesting that indeed these vertical C_2's serve as the precursor for the nucleation of graphite, and perhaps also for diamond.

91 2 04 095

20. DISTRIBUTION / AVAILABILITY OF ABSTRACT	21. ABSTRACT SECURITY CLASSIFICATION
☒ UNCLASSIFIED/UNLIMITED ☒ SAME AS RPT. ☐ DTIC USERS	Unclassified

22a. NAME OF RESPONSIBLE INDIVIDUAL	22b. TELEPHONE (Include Area Code)	22c. OFFICE SYMBOL
Dr. Mark Ross	(202) 696-4409	

DD FORM 1473, 84 MAR   83 APR edition may be used until exhausted.   SECURITY CLASSIFICATION OF THIS PAGE
All other editions are obsolete.

Unclassified

OFFICE OF NAVAL RESEARCH

Contract N00014-89-J-1103

R & T Code 4134043-01

Technical Report No. 58

CEELS as a Probe of the Carbide to Graphite Transformation on NI

By

DAVID E. RAMAKER

Prepared for Publication

in

Proc. 2nd. Intn. Conf. New Diamond Sci. & Tech. (Mat. Res. Soc.)

George Washington University
Department of Chemistry
Washington, D.C.

January, 1991

CEELS AS A PROBE OF THE CARBIDE TO GRAPHITE TRANSFORMATION ON Ni

David E. Ramaker[*]

Chemistry Division, Naval Research Laboratory, Washington, DC. 20375, USA

ABSTRACT

Recent effective medium theory calculations indicate that a nucleation step must be involved in the carbide to graphite transformation on Ni, and that vertical C_2 may be a precursor to this nucleation step. A similar nucleation site could also be involved in diamond formation on metals. We interpret previously published C K edge CEELS and NEXAFS data for carbon/Ni between 500-700K. We make comparison with theoretical DOS calculations, and utilize CEELS angle dependencies to assign features and determine bond orientations on the surface. The results confirm that horizontal C_n, most likely C_2, exists on the surface up 600K, but that at 620K, some of the C_2 species flip up. Evidence for vertical C_2 is seen only at higher C coverages suggesting that indeed these vertical C_2's serve as the precursor for the nucleation of graphite, and perhaps also for diamond.

THE CARBIDE TO GRAPHITE TRANSFORMATION

Carbon is relatively unreactive with Ni. Thus Ni forms a relatively unstable carbide, which above 670K either undergoes dissolution into the bulk or at higher coverages forms a graphitic layer which sits high above the surface (e.g. 2.8 Å above a Ni(111) surface) [1]. Recent calculations utilizing effective medium theory (EMT) [1] shed some light on this transformation. In the EMT approach, the atom positions are determined by the electron density, each atom seeking its own unique optimum density. These calculations conclude that at intermediate coverage, the C-C interaction drives carbon closer to a Ni surface, but in a graphite layer, the C-C interaction drives carbon away from the surface. They conclude that the carbide to graphite evolution is discontinuous, indicating that a nucleation step must be involved.

The calculations also suggest that horizontal C_2 species on a Ni(111) surface are not stable at high temperature, but that vertical (i.e. perpendicular) C_2 species may be stable on the Ni surface [1]. However, this vertical C_2 is too close to the surface to serve as a nucleation site for graphite formation by itself. A C_3 species is the smallest entity which moves sufficiently far from the Ni surface to serve as a graphite nucleation site. Darling et al. [1] then postulate that a vertical C_2 species may either "tip over" to form a C_3 species, which moves

away from the surface to act as a graphite nucleation site, or a graphitic layer forms on top of a carbidic layer (i.e. the outer C of the vertical C_2 may become part of the graphite layer, and the inner C may ultimately undergo dissolution into the bulk). In either case, a vertical C_2 serves as a precursor to the nucleation site.

An identical nucleation step could be involved in the nucleation of diamond on metal surfaces, and critically determine the bonding of the diamond film to the metal. Thus we search for experimental confirmation of these theoretical results for graphite. NEXAFS (near edge x-ray absorption fine structure) data have been very helpful in determining the various orientations of molecular hydrocarbon fragments on Ni below 450 K [2], but little new information from NEXAFS data has been obtained for C/Ni above 450 K. In this work we utilize previously published [3,4] CEELS (core electron energy loss spectroscopy) and NEXAFS data [5] to obtain experimental verification that vertical C_2 acts as a precursor for graphite nucleation on Ni.

Recently Caputi et al. [3] reported AES and CEELS data for carbon on Ni(100) in the range 520-770 K. Core-level and valence band XPS data have also been reported [3]. A detailed interpretation of the AES and XPS data has revealed extensive C-C bonding on the surface, in what was previously believed to be carbidic (i.e. only C-M bonding) in character [6]. At higher temperatures, just prior to the formation of graphite around 620K, the AES data indicate that the amount of C-C bonding appears to decrease. No meaningful interpretation of the CEELS data in this same temperature range has been reported.

CEELS ANGULAR DEPENDENCE

In NEXAFS, the dipole selection rule (i.e. s → p only) is appropriate. By CEELS, we mean the use of small electron energies (500-1000 eV) and the measurement of back scattered electrons which have suffered large momentum transfer, in which case the validity of the dipole selection rule is not expected. Thus optically forbidden monopole transitions should be evident. Nevertheless, CEELS data can still be utilized to obtain some of the same information obtainable from NEXAFS data.

We utilize equations derived by Cheung [7] for determining the angular dependence of CEELS data for graphite, which has the σ orbital parallel to the surface. Cheung obtains,

$$\{1s \rightarrow \pi\} \quad \propto \quad 1.5\xi\sin^2\delta \quad + \quad 3\nu[\cos^2\delta - 0.5\sin^2\delta]\sin^2\theta \qquad (1)$$

$$\{1s \rightarrow \sigma\} \quad \propto \quad \xi/3 + \nu[1-0.5\sin^2\delta] - \nu[\cos^2\delta - 0.5\sin^2\delta]\sin^2\theta, \qquad (2)$$

where δ is the electron acceptance angle and ξ and ν are the magnitude of the monopole and dipole contributions, respectively. Here θ is the angle between

the surface and the electron beam direction. We compare these expressions with those appropriate for NEXAFS and C=C bonds parallel to the surface [2],

$$\{1s \rightarrow \pi\} \quad \propto \quad 6\cos^2\theta \tag{3}$$

$$\{1s \rightarrow \sigma\} \quad \propto \quad 3\sin^2\theta. \tag{4}$$

If we assume that $\delta = 90^\circ$ in eqs. 1 and 2 (i.e. that electrons are counted at all acceptance angles), the CEELS technique mimics the NEXAFS technique, which utilizes the total electron yield or the Auger yield. We then obtain,

$$\{1s \rightarrow \pi\} \quad \propto \quad 1.5\nu \cos^2\theta \tag{5}$$

$$\{1s \rightarrow \sigma\} \quad \propto \quad \xi/3 + 0.5\nu + 0.5\nu \sin^2\theta. \tag{6}$$

These expressions have similar $\sin^2\theta$ and $\cos^2\theta$ dependences to those above for NEXAFS as expected. In contrast, if we assume $\delta = 16.5^\circ$ (i.e. the appropriate acceptance angle for a cylindrical mirror analyzer and a 500 eV excitation beam as utilized by Cheung [7]), we obtain the expressions,

$$\{1s \rightarrow \pi\} \quad \propto \quad 0.12\nu + 2.64\nu \sin^2\theta \tag{7}$$

$$\{1s \rightarrow \sigma\} \quad \propto \quad \xi/3 + 0.08\nu + 0.88\nu \cos^2\theta. \tag{8}$$

Notice the switch in $\cos^2\theta / \sin^2\theta$ dependence between eqs. 5, 6 and 7, 8. Eqs. 7 and 8, appropriate for this case, are also different from that for NEXAFS, eqs. 3 and 4. Furthermore, Cheung [7] found empirically for graphite with a 500 eV excitation beam that ξ/ν is about 8. Thus in CEELS for $\theta = 90^\circ$ (i.e. electron beam perpendicular to surface, which is generally the case for the data discussed in this work) the π and σ contributions have nearly equal intensity (eqs. 7 and 8 above both give 2.75ν). If the C-C bond is vertical to the surface, we expect a corresponding reversal in the dipole intensity dependencies giving $\{1s \rightarrow \pi\} = 0.08\nu$ and $\{1s \rightarrow \sigma\} = 5.42\nu$.

In summary, the CEELS data should give about equal σ and π area intensities for parallel C-C orientation, and be dominated by σ intensity for perpendicular C-C orientation.

INTERPRETATION OF CEELS FEATURES

Figs. 1b and c compare $-d^2N(E)/dE^2$ K edge CEELS curves for various carbonaceous layers on metals [3,4] along with NEXAFS data for CO/Ni(100) at 670K in 1d [5]. We have also included in Fig. 1a NEXAFS [8] data for condensed benzene and cyclohexane for comparison. NEXAFS data for a large number of molecules and solids show C-H and C-C π^* and σ^* features at surprisingly specific energies [8]; so we have labelled these features accordingly in Fig. 1a.

All of the carbonaceous layers were prepared by exposure of the Ni surfaces to CO at around 500K, and then heating. The dashed curve in 1b was
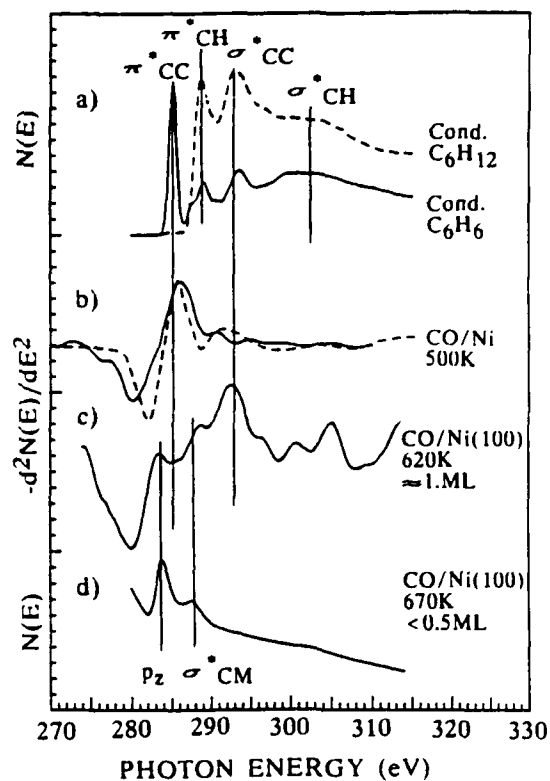
Fig. 1

a) C K NEXAFS data for condensed benzene and cyclohexane [5],

b) $-d^2N(E)/dE^2$ C K edge CEELS data for CO/Ni(100) at 500K (dotted line) [3] and CO/Ni(111) at 520K (solid line [4]),

c) CEELS data for CO/Ni(100) at 620K [3], and

d) NEXAFS data for CO/Ni(100) at 670K, but at low coverage [5].

reported by Rosei et al [4] for a Ni(111) surface upon heating to 500K with an estimated coverage of about 0.3 ML (this is a very crude estimate). The solid curves in b (at 520K) and c (at 620K) were reported by Caputi et al [3]. Although *they do not estimate the C coverage, it is believed to be greater than or equal to 1 ML.* The NEXAFS curve in (d) was reported by Stohr and Jaeger [5] with incident angle $\vartheta = 20^o$. Consistent with the expected NEXAFS angular dependence, this curve emphasizes vertical σ bonds. The latter curve corresponds to less than 0.5 ML of "carbidic" C on the surface. The K binding energy is about 282.9 eV for a carbidic layer on Ni(100) [9]. We have deconvoluted the Caputi data by a 2 eV Gaussian line shape to regain better resolution since it was taken with a large 6 V_{ptp} modulation voltage.

The deconvolved Caputi data on Ni(100) and the Rosei data on Ni(111) at 500 K are quite similar as expected. They reveal the characteristic π^*_{CC} and σ^*_{CC} peaks at 285 eV and 293 eV respectively as seen in the molecular NEXAFS data. Since C-M bonds do not produce peaks in this energy range [10], this clearly indicates the presence of C-C bonding on the surface, consistent with the AES and XPS data [6] as indicated above. The similar area intensities of the π^*_{CC} and σ^*_{CC} peaks indicate that the C-C bonds lie flat on the surface. We would assume that these C-C bonds primarily exist as C_n (n = 2,3 etc, with n = 2 favored) species on the surface.

The Caputi data at 620K (curve c) reveal dramatic differences from that at 520K. Now the σ^*_{CC} feature dominates with the π^*_{CC} feature nearly missing. This is consistent with C-C bonds perpendicular to the surface. We believe the σ^*_{CC} feature now arises from C_2 species standing erect on the surface.

NEXAFS data for CO/Ni(100) at 300 K [5] (not shown) are dominated by the π^* and σ^* CO bond features. Heating to 670K breaks all C-O bonds, leaving only atomic C on the surface. Notice that in Fig. 2d, no evidence exist for either C-O or C-C bonds. The features at 284 and 288 eV are attributed [10] to nonbonding p_z orbitals and σ^*_{CM} orbitals bonding the atomic C to the surface. Evidence for these same features also exists in the deconvolved 620K data of Caputi (curve 1c).

COMPARISON WITH THEORETICAL DOS

Fig. 2 provides further evidence for our assignment of the p_z and σ^*_{CM} features above. We compare NEXAFS data for NbC [11] and C/Ni (i.e. the data in Fig. 1) to DOS results for NbC reported by Schwarz [12] and for C/Ru reported by Feibelman [13]. Schwarz utilized a self-consistent augmented plane wave (APW) X_α calculation for a periodic NbC solid. Feibelman's results were obtained for a (1x1) overlayer of C atoms on an 11-layer Ru(0001) film, with only 1/3 of the three-fold sites filled with carbon atoms. In this theoretical model, the carbon atoms are relatively isolated since the nearest C-C distance is greater than 5.0 a.u. compared with a C-C distance of 2.68 a.u. in graphite [13]. We believe Feibelman's results should be adequate for low coverages of C/Ni since both Ru and Ni form relatively unstable carbides compared with Nb or Ti.

The DOS from both calculations are available for only the first 10 eV or less of the conduction band.. Schwarz identified the two peaks in the DOS as the π^* and σ^* antibonding features (i.e. involving the t_{2g} and e_g Nb d orbitals). Feibelman identified the two major peaks for C/Ni as the p_z and σ^* features.

Fig. 2

Comparison of C K NEXAFS data for NbC and C/Ni with DOS calculations.

a)   NEXAFS data from Wesner et al [11], shifted up in energy by 3.0 eV based on calibration with similar data for graphite. DOS calculation from Schwarz [12].

b) NEXAFS data from Stohr and Jaeger [5] for CO/Ni at 670K with DOS from Feibelman for a (1x1) layer of C on a Ru(0001) film.
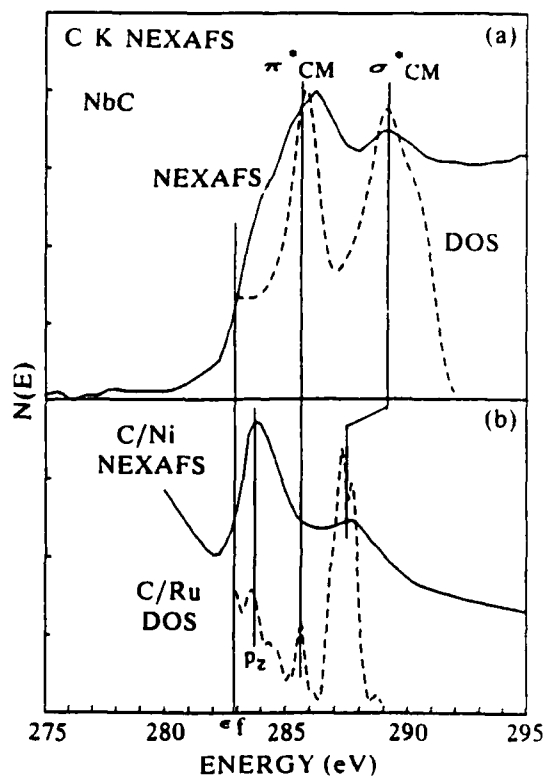
The p_z feature arises from the C nonbonding or "dangling" bonds pointing outward from the surface. The σ^* feature arises from the three sp^3-like C-metal bonds per C atom. Note that a similar π^* feature also appears in Feibelman's DOS and aligns with the same peak for NbC, but it has much weaker intensity. Furthermore, note that the σ^* feature has a much lower energy for C/Ni than for NbC. This reflects the much weaker C-metal interaction in Ni-C bonds compared with Nb-C. The comparison with the DOS also helps to identify the precise position of the Fermi level. We place the Fermi level at 282.9 eV.

CONCLUSIONS

In summary, our interpretation of the spectroscopic results are consistent with our previous interpretations of the AES and XPS data [6], and with Darling's EMT theoretical results as discussed above [1]. First, the CEELS data do indeed verify that significant horizontal C-C bonding exists on the surface below 600K. We anticipate that this is in the form of C_n. Around 620K, some vertical C_2 is formed along with considerable C_1 (i.e. atomic C). However, the CEELS and NEXAFS data also suggest that vertical C_2 is formed only at higher coverages (it is clearly present in the Caputi data [coverage about 1 ML] but absent in Stohr and Jaeger's NEXAFS data [coverage < 0.5 ML]). At higher coverages, we envisage that some of the C_2 are forced to flip up to make room for the neighboring horizontal C_2's to dissociate. These vertical C_2's may then serve as the precursor for the nucleation of graphite, since it would explain the lack of graphite formation from C_2H_4/Ni(100) (i.e. at low carbon coverages). Further exposure to C_2H_2 at higher temperatures (i.e. producing higher C coverages) does lead to graphite formation on Ni(100) [9]. Thus we provide the first experimental evidence for vertical C_2 as a precursor for graphite nucleation and corroborate the theoretical EMT [1] results.

REFERENCES

1. G.R. Darling, J.B. Pendry, and R.W. Joyner, Surf. Sci. 221, 69 (1989).
2. J.A. Horsley, J. Stohr, and R.J. Koestner, J. Chem. Phys. 83, 3146 (1985).
3. L.S. Caputi, G. Chiarello, and L. Papagno, Surf. Sci. 162, 259 (1985).
4. R. Rosei, S. Modesti, F. Sette, C. Quaresima, A. Savoia, and P. Perfetti, Phys. Rev. B29, 3416 (1984).
5. J. Stohr and R. Jaeger, Phys. Rev. B26, 4111 (1982).
6. F.L. Hutson, D.E. Ramaker, and B.E. Koel, submitted to Surf. Sci.
7. T.T.P. Cheung, Phys. Rev. B31, 4792 (1985).
8. D.A Outka and J. Stohr, in Chemistry and Physics of Solid Surfaces VII", edited by R.Vanselow and R. Howe (Springer-Verlag, Heidelberg, 1988), p.20.
9. S.C. Gebhard and B.E. Koel (unpublished).
10. D.E. Ramaker and F.L. Hutson, submitted to Phys. Rev. B.
11. D. Wesner, S. Krummacher, M. Strongin, R. Carr, T.K. Sham, W. Eberhardt and S.L. Weng, Phys. Rev. B30, 855, 1984.
12. K. Schwarz, J. Phys. C: Solid State Phys. 10, 195 (1977); 8, 809 (1975).
13. P.J. Feibelman, Phys. Rev. B26, 5347 (1982).

TECHNICAL REPORT DISTRIBUTION LIST - GENERAL

Office of Naval Research   (2)
Chemistry Division, Code 1113
800 North Quincy Street
Arlington, Virginia 22217-5000

Dr. Robert Green, Director   (1)
Chemistry Division, Code 385
Naval Weapons Center
China Lake, CA 93555-6001

Commanding Officer   (1)
Naval Weapons Support Center
Dr. Bernard E. Douda
Crane, Indiana 47522-5050

Chief of Naval Research   (1)
Special Assistant for Marine
   Corps Matters
Code 00MC
800 North Quincy Street
Arlington, VA 22217-5000

Dr. Richard W. Drisko   (1)
Naval Civil Engineering
 Laboratory
Code L52
Port Hueneme, CA 93043

Dr. Bernadette Eichinger   (1)
Naval Ship Systems Engineering
   Station
Code 053
Philadelphia Naval Base
Philadelphia, PA 19112

David Taylor Research Center (1)
Dr. Eugene C. Fischer
Annapolis, MD 21402-5067

Dr. Sachio Yamamoto   (1)
Naval Ocean Systems Center
Code 52
San Diego, CA 92152-5000

Dr. James S. Murday   (1)
Chemistry Division, Code 6100
Naval Research Laboratory
Washington, D.C. 20375-5000

Dr. Harold H. Singerman   (1)
David Taylor Research Center
Code 283
Annapolis, MD 21402-5067

Defense Technical Information Center
Building 5, Cameron Station
Alexandria, VA   22314

Professor John Baldeschwieler
Department of Chemistry
California Inst. of Technology
Pasadena, CA 91125

Professor Paul Barbara
Department of Chemistry
University of Minnesota
Minneapolis, MN 55455-0431

Dr. Duncan Brown
Advanced Technology Materials
520-B Danury Rd.
New Milford, CT 06776

Professor Stanley Bruckenstein
Department of Chemistry
State University of New York
Buffalo, NY 14214

Professor Carolyn Cassady
Department of Chemistry
Miami University
Oxford, OH 45056

Professor R.P.H. Chang
Dept. Matls. Sci. & Engineering
Northwestern University
Evanston, IL 60208

Professor Frank DiSalvo
Department of Chemistry
Cornell University
Ithaca, NY 14853

Dr. James Duncan
Federal Systems Division
Eastman Kodak Company
Rochester, NY 14650-2156

Professor Arthur Ellis
Department of Chemistry
University of Wisconsin
Madison, WI 53706

Professor Mustafa El-Sayed
Department of Chemistry
University of California
Los Angeles, CA 90024

Professor John Eyler
Department of Chemistry
University of Florida
Gainesville, FL 32611

Professor James Garvey
Department of Chemistry
State University of New York
Buffalo, NY 14214

Professor Steven George
Department of Chemistry
Stanford University
Stanford, CA 94305

Professor Tom George
Dept. of Chemistry & Physics
State University of New York
Buffalo, NY 14260

Dr. Robert Hamers
IBM T.J. Watson Research Center
P.O. Box 218
Yorktown Heights, NY 10598

Professor Paul Hansma
Department of Physics
University of California
Santa Barbara, CA 93106

Professor Charles Harris
Department of Chemistry
University of California
Berkeley, CA 94720

Professor John Hemminger
Department of Chemistry
University of California
Irvine, CA 92717

Professor Roald Hoffmann
Department of Chemistry
Cornell University
Ithaca, NY 14853

Professor Leonard Interrante
Department of Chemistry
Rensselaer Polytechnic Institute
Troy, NY 12181

Professor Eugene Irene
Department of Chemistry
University of North Carolina
Chapel Hill, NC 27514

Dr. Sylvia Johnson
SRI International
333 Ravenswood Avenue
Menlo Park, CA 94025

Dr. Zakya Kafafi
Code 6551
Naval Research Laboratory
Washington, DC 20375-5000

Professor Larry Kesmodel
Department of Physics
Indiana University
Bloomington, IN 47403

Professor Max Lagally
Dept. Metal. & Min. Engineering
University of Wisconsin
Madison, WI   53706

Dr. Stephen Lieberman
Code 522
Naval Ocean Systems Center
San Diego, CA   92152

Professor M.C. Lin
Department of Chemistry
Emory University
Atlanta, GA   30322

Professor Fred McLafferty
Department of Chemistry
Cornell University
Ithaca, NY   14853-1301

Professor Horia Metiu
Department of Chemistry
University of California
Santa Barbara, CA   93106

Professor Larry Miller
Department of Chemistry
University of Minnesota
Minneapolis, MN   55455-0431

Professor George Morrison
Department of Chemistry
Cornell University
Ithaca, NY   14853

Professor Daniel Neumark
Department of Chemistry
University of California
Berkeley, CA   94720

Professor David Ramaker
Department of Chemistry
George Washington University
Washington, DC   20052

Dr. Gary Rubloff
IBM T.J. Watson Research Center
P.O. Box 218
Yorktown Heights, NY   10598

Professor Richard Smalley
Department of Chemistry
Rice University
P.O. Box 1892
Houston, TX   77251

Professor Gerald Stringfellow
Dept. of Matls. Sci. & Engineering
University of Utah
Salt Lake City, UT   84112

Professor Galen Stucky
Department of Chemistry
University of California
Santa Barbara, CA   93106

Professor H. Tachikawa
Department of Chemistry
Jackson State University
Jackson, MI   39217-0510

Professor William Unertl
Lab. for Surface Sci. & Technology
University of Maine
Orono, ME   04469

Dr. Terrell Vanderah
Code 3854
Naval Weapons Center
China Lake, CA   93555

Professor John Weaver
Dept. of Chem. & Mat. Sciences
University of Minnesota
Minneapolis, MN   55455

Professor Brad Weiner
Department of Chemistry
University of Puerto Rico
Rio Piedras, Puerto Rico   00931

Professor Robert Whetten
Department of Chemistry
University of California
Los Angeles, CA   90024

Professor R. Stanley Williams
Department of Chemistry
University of California
Los Angeles, CA   90024

Professor Nicholas Winograd
Department of Chemistry
Pennsylvania State University
University Park, PA   16802

Professor Aaron Wold
Department of Chemistry
Brown University
Providence, RI   02912

Professor Vicki Wysocki
Department of Chemistry
Virginia Commonwealth University
Richmond, VA   23284-2006

Professor John Yates
Department of Chemistry
University of Pittsburgh
Pittsburgh, PA   15260